Thermochimica Acta, 165 (1990) 85–91
Elsevier Science Publishers B.V., Amsterdam

THE REDUCTION OF V_2O_5. PART II. REDUCTION BY HYDROGEN

F. STANDER

Council for Mineral Technology, Private Bag X3015, Randburg 2125 (South Africa)

C.P.J. VAN VUUREN *

Department of Materials Science and Metallurgical Engineering, University of Pretoria, Pretoria 0002 (South Africa)

(Received 21 December 1989)

ABSTRACT

The reduction of V_2O_5 by H_2 was studied and compared with the results obtained for the reaction of V_2O_5 with CO. The reaction was found to be exothermic and various intermediate oxides were formed during the course of the reaction. The oxides with general composition V_nO_{2n-1} with $4 \leq n \leq 8$ seem to be the intermediates formed. The rate of reduction was found to be faster in the H_2 than in the CO atmosphere. The sample morphology seems to influence the rate of reduction as well: the powder sample was found to react more slowly than the platelets at temperatures below 460 °C; above 460 °C, the platelets reacted more slowly than the powder samples. The Avrami–Erove'ev equation with $n = 4$ seems to describe the reduction of the powder while the reaction of the platelets is described by a first-order kinetic equation.

INTRODUCTION

The reduction of V_2O_5 to V_2O_3 with CO was described in Part I of this series [1]. It was shown that the intermediate oxides, V_6O_{13} and VO_2, are formed during the reduction reaction. Hydrogen gas is a reducing agent with important industrial applications. It was therefore important to obtain experimental data of the reaction with H_2 as reducing agent and to compare it with that obtained for CO.

EXPERIMENTAL

The experimental procedures which were followed were described in Part I [1]. It is important to note that the experimental conditions such as sample

* Author to whom correspondence should be addressed.

0040-6031/90/$03.50

size (20–30 mg), grain morphology of the V_2O_5, isothermal temperatures and gas flow rates were the same as those which were used in the CO reduction process. The only difference was that a Du Pont 990 thermal analyser with a 951 TGA-module, instead of the Stanton Redcroft 951 thermal analyser, was used to collect the TG data.

RESULTS AND DISCUSSION

Dynamic thermal analysis

The TG and DTA curves of the reduction of V_2O_5 powder by H_2 are given in Fig. 1. At a heating rate of 10 °C min^{-1}, only a single exotherm is visible in the 450–650 °C temperature range. The experimental mass loss as observed on the thermobalance was 17.3%, which is in fair agreement with the calculated value of 17.59% if the final product is V_2O_3. X-ray powder diffraction confirmed that V_2O_3 was the final product.

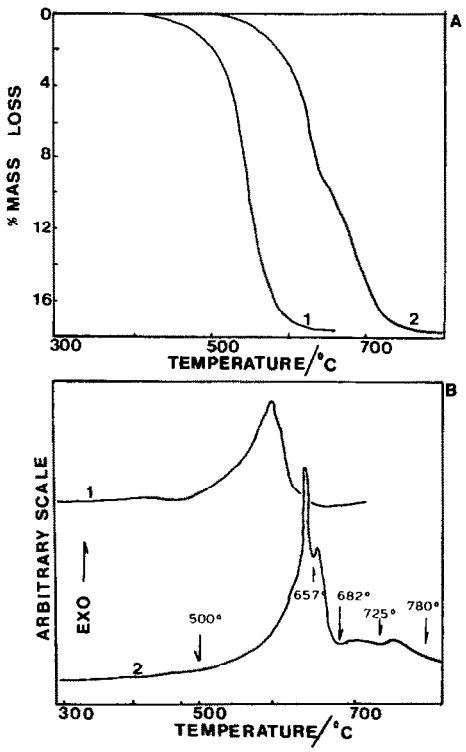

Fig. 1. TG (A) and DTA (B) curves for the reduction of V_2O_5 powder by hydrogen: curve 1, heating rate 10 °C min^{-1}; curve 2, heating rate 50 °C min^{-1}.

TABLE 1

Vanadium oxide phases detected by X-ray powder diffraction during the hydrogen reduction of V_2O_5

Temperature (°C)	V_2O_5	V_6O_{13}	VO_2 (rutile)	V_nO_{2n-1} $(4 \leq n \leq 8)$	V_2O_3
500	s	n.o.	n.o.	n.o.	n.o.
657	w	s	w	n.o.	n.o.
682	n.o.	n.o.	s	n.o.	n.o.
725	n.o.	n.o.	w	w	n.o.
780	n.o.	n.o.	n.o.	n.o.	s

Abbreviations: s, high intensity peaks; w, weak intensity peaks; n.o. = not observed.

At a higher heating rate, 50 °C min^{-1}, two steps are clearly visible on the TG curve. The first step corresponds to the formation of VO_2 and the second to that of V_2O_3. The DTA curve, however, shows four overlapping

TABLE 2

Observed X-ray powder diffraction peaks for the reduction of V_2O_5 at 725 °C

Observed peaks d (Å) (I/I_1)	Possible corresponding oxide peaks d (Å) (I/I_1)					
	VO_2	V_4O_7	V_5O_9	V_6O_{11}	V_7O_{13}	V_8O_{15}
3.84–3.56		3.70		3.83	3.73	3.65
(25)		(40)		(60)	(60)	(60)
3.33–3.29	3.31	3.33	3.32	3.31	3.30	3.29
(100)	(30)	(100)	(100)	(100)	(100)	(100)
3.21–3.15	3.20			3.19		
(50)	(100)			(40)		
3.11–2.91		3.05	3.03	3.06	3.08	3.09
(40–50)		(40)	(60)	(100)	(100)	(100)
		2.97		2.93	2.97	2.99
		(60)		(100)	(100)	(100)
2.47–2.41	2.43	2.48	2.46	2.45		2.44
(40–50)	(60)	(60)	(60)	(60)		(60)
		2.42	2.42	2.42	2.42	2.42
		(60)	(60)	(60)	(60)	(60)
2.35–2.33			2.36	2.35	2.34	2.35
(25)			(40)	(40)	(40)	(40)
				2.33	2.33	
				(40)	(40)	
2.21–2.14		2.82	2.12	2.20	2.16	2.16
(35)		(100)	(40)	(40)	(60)	(100)
			2.17	2.17	2.15	2.16
			(60)	(60)	(60)	(60)
			2.16	2.16		2.15
			(40)	(60)		(60)

exotherms. The reaction was terminated at various temperatures, which roughly corresponded to valleys on the DTA curve recorded at 50 °C min^{-1} (see curve 2, Fig. 1). The sample was cooled to ambient temperature in an argon atmosphere and analysed using X-ray powder diffraction. The results are summarised in Table 1.

The oxides with composition V_nO_{2n-1} ($4 \leq n \leq 8$) are members of a homologous series of oxides with a limited stability range [2]. These oxides were not detected during the reduction with CO but their formation cannot be excluded. The structures of all these oxides are based on rutile. Their X-ray powder diffraction patterns are very similar and it was therefore very difficult to distinguish between them, especially with the low-resolution X-ray powder diffractometer which was available. The diffraction pattern consisted of broad bands which are probably the result of a number of overlapping peaks. Table 2 gives a summary of the *d*-spacing intervals as observed for these bands together with corresponding literature (ASTM) values for the various oxides. A number of structures with composition VO_2 have been described in the literature [3–5]. The VO_2 phase detected in this study corresponds to that described by Anderson [3]. This oxide has a

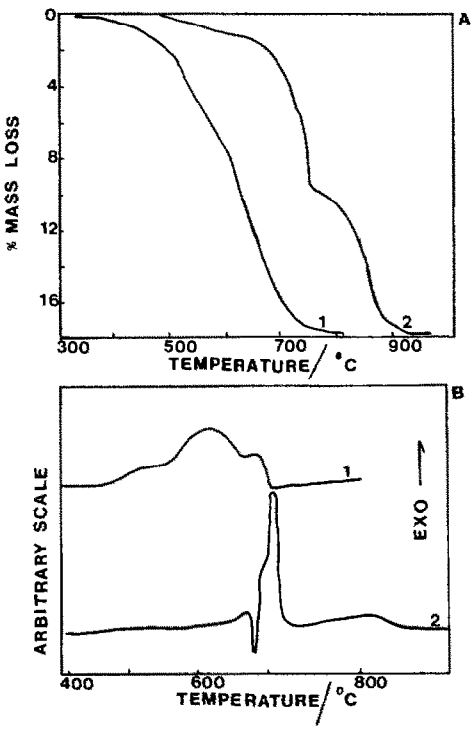

Fig. 2. TG (A) and DTA (B) curves for the reduction of V_2O_5 platelets by hydrogen: curve 1, heating rate 10 °C min^{-1}; curve 2, heating rate 50 °C min^{-1}.

monoclinic structure consisting of an array of V_2O_4 units with a slightly distorted rutile lattice.

The TG and DTA curves for the reduction of the platelets by H_2 are given in Fig. 2. The reduction of the platelets, as compared to the powder, is completed at higher temperatures. This tendency was also observed for the reduction process with CO. The DTA curves indicate overlapping exothermic reactions. The same intermediates as those described for the reduction of the powder were detected. The endothermic peak at approximately 670 °C (heating rate 50 °C min^{-1}) can be assigned to the melting of V_2O_5.

Isothermal thermal analysis

The total mass losses recorded on the isothermal TG reduction curves for the V_2O_5 powder and platelets corresponded to the formation of V_2O_3. An increase in isothermal temperature of the powder resulted in an increase in reduction rate. This is illustrated in Fig. 3. The rate of reduction of the platelets at temperatures below 460 °C was found to be faster than that of the powder. This effect was also observed for the reduction reaction with CO and is contrary to expectation as the surface area of the platelets (< 0.5 m^2 g^{-1}) was much smaller than that of the powder (2.87 m^2 g^{-1}). The reduction rate of the platelets seems to level off between 450 and 460 °C but starts to show an increase with temperature again above 480 °C. This effect was not as pronounced as was observed for the CO reduction reaction. A similar effect was observed for the reduction of Fe_2O_3 with CO and H_2: it was thought to be due to the sintering of the material which produced a layer which impeded the diffusion of the water vapour and CO_2 away from the reaction site and thus slowed the reaction down [6]. In general, however, the reduction reaction was found to be much faster in an H_2 than in a CO atmosphere. This is illustrated in Fig. 4.

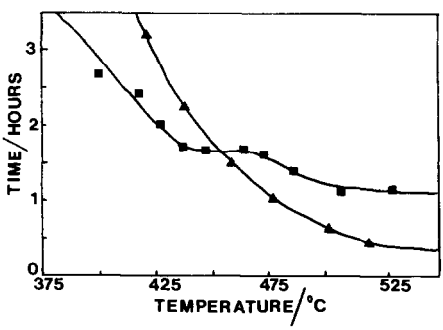

Fig. 3. Reduction time as a function of the isothermal temperature for V_2O_5 powder (▲) and platelets (■).

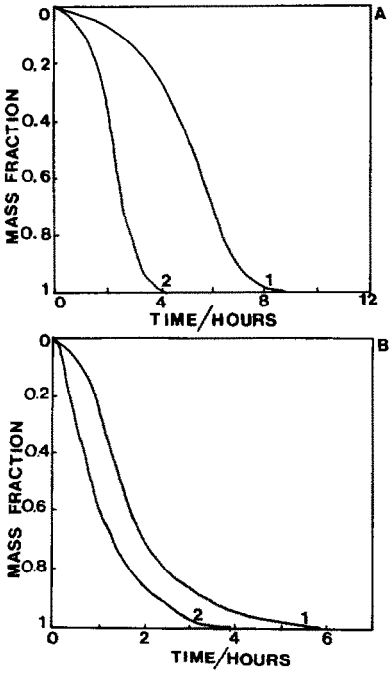

Fig. 4. Isothermal TG reduction curves for V_2O_5 powder (A) and platelets (B): curve 1, reduction by CO; curve 2, reduction by H_2.

Kinetic analysis of the reduction reaction

The experimental isothermal rate data which were collected between 400 and 520 °C for the powder and platelet samples were fitted to various kinetic models. The data for the powder sample fitted the Avrami–Erofe'ev equation, $[-\ln(1-\alpha)]^{1/4} = k(t - t_0)$. This kinetic model was also found to describe the reduction reaction of the powder with CO. An apparent activation energy of 77.4 kJ mol^{-1} and ln A (s^{-1}) = 3.94, cf. E_a = 64.5 kJ mol^{-1} and ln A (s^{-1}) = 0.99 for CO, was calculated from an Arrhenius plot.

The reduction of the platelets was found to be described by the first-order kinetic equation, $[-\ln(1-\alpha)] = k(t - t_0)$, which is different from the nucleation and growth model, the Avrami–Erofe'ev equation with $n = 2$, which described the CO reduction reaction. An apparent activation energy of 33.2 kJ mol^{-1} was calculated for this reaction. It is, however, necessary to recognise that more complementary experimental data, such as microscopy data, are needed in order to understand the physical significance of these parameters.

ACKNOWLEDGEMENTS

The authors thank the University of Pretoria, the Council for Metal Technology and the Foundation for Research and Development for financial assistance.

REFERENCES

1 C.P.J. van Vuuren and F. Stander, Thermochim. Acta, 165 (1990) 73.
2 J. Stringer, J. Less-Common Met., 8 (1986) 1.
3 G. Andersson, Acta Chem. Scand., 10 (1956) 623.
4 F. Thèobald, R. Cabala and J. Bernard, J. Solid State Chem., 17 (1976) 431.
5 S. Horiuchi, M. Saeki, Y. Matsui and F. Nagata, Acta Crystallogr. A, 31 (1975) 660.
6 C.B. Alcock, Principles of Pyrometallurgy, Academic Press, London, 1978, p. 85.